THE EFFECT OF VOLUME FRACTION OF SiO_2 NANOPARTICLE ON FLOW AND HEAT TRANSFER CHARACTERISTICS IN A DUCT WITH CORRUGATED BACKWARD-FACING STEP

by

Recep EKICILER[a*], Emre AYDENIZ[b], and Kamil ARSLAN[b]

[a] Department of Mechanical Engineering, Gazi University, Ankara, Turkey
[b] Department of Mechanical Engineering, Karabuk University, Karabuk, Turkey

Original scientific paper
https://doi.org/10.2298/TSCI18S5435E

In this paper, flow and heat transfer characteristics of SiO_2-water nanofluid flow over a corrugated backward-facing step are numerically investigated. The numerical study is performed by solving governing equations (continuity, momentum, and energy) with finite volume method. The duct inlet and step heights are 4.8 mm. The expansion ratio is 2. The upstream wall, L_u, and downstream wall, L_d, lengths are 48 cm and 96 cm, respectively. The downstream wall of the duct is subjected to a constant and uniform heat flux of 2000 W/m^2. The ranges of the volume fraction of nanoparticles and Reynolds number are 0%-3.0% and 135-240, respectively. The effects of the volume fraction of nanoparticles on the average Nusselt number, average Darcy friction factor, and velocity distribution are investigated under laminar forced convective nanofluid flow condition. It is revealed that the nanoparticle volume fraction substantially influences the heat transfer and flow characteristics. The volume fraction of 3.0% shows the highest heat transfer performance.

Key words: *backward-facing step, re-circulation region, corrugated duct, forced convection, nanofluid*

Introduction

Flow separation and re-attachment of the fluid caused by sudden expansion is important in many engineering applications. Heat transfer applications of backward-facing step (BFS) are mainly used in avionics systems, high performance heat exchangers, wide-angle diffusers, cooling of nuclear reactors, airfoils, electronic cooling equipment, combustion chambers, cooling of turbine blades, environmental control systems, axial and centrifugal compressor blades, and are also used in many other heat transfer devices [1-4].

In the literature, the separation and re-attachment flow over a BFS was firstly carried out in the 1950's. Studies on separated flow have been researched more extensively by increasing popularity over in the last decade. Goldstein *et al.* [5] performed an experimental study to investigate the re-attachment point under laminar and subsonic flow conditions over a step. They noticed that the re-attachment point and boundary displacement thickness change with Reynolds number. Denham and Patrick [6] investigated 2-D laminar flow over the BFS. Water was used as a working fluid. The channel's expansion and aspect ratios were equal to 3 and 20, respectively. The Reynolds number was varied between 50-250. They observed that

* Corresponding author, e-mail: recepekiciler@gazi.edu.tr

flow characteristics of BFS are similar to the other 2-D geometries having sudden expansion. Yet, both re-circulation length and mass-flow rate were smaller. At Re = 229, they noticed a fluctuation, which shows the beginning of the transition to the turbulent separated boundary--layer. Rinoie *et al.* [7] experimentally investigated turbulent flow over the BFS to clarify the behavior of turbulent flow inside the re-attachment shear layer using turbulent energy balance assisting in the understanding of the turbulent flow of BFS. Step height and aspect ratio were 0.02 m and 10 m, respectively. They observed that turbulent structures can be classified in three categories (the dead air, reversed flow, and separated shear layer zone). In the turbulent energy balance, transverse diffusion assisting to balance the dissipation term was positive. Nie and Armally [8] examined numerically the effects of step height on heat transfer and flow characteristics in a 3-D BFS channel. The flow was thought as laminar and forced convection conditions. Air was passed through the channel as working fluid. Thermophysical properties of air were assumed constant along the channel. The study was performed at constant Reynolds number (Re = 343). Constant and uniform heat flux, $q''_w = 50$ W/m^2, was subjected to downward of the step wall while the other walls were insulated. Three different step heights were performed in this study. They observed at the end of the study that Nusselt number, general 3-D flow characteristic feature, and gradient locating in the re-circulation region increases with increasing step height. Also, they noticed that step height effects the friction coefficient distribution. Xie and Xi [9] studied a numerical analysis of heat transfer characteristic on BFS. The air was selected as a working fluid. Reynolds number was varied between 400-1000. Expansion ratio was set such as 1.5, 2.0, and 2.5. Inlet temperature and bottom wall temperature were 10 °C and 40 °C, respectively. They obtained that Nusselt number increases with increasing of Reynolds number. Also, the Nusselt number increases with increasing the expansion ratio. Xu *et al.* [10] performed a numerical study to understand the effect of Reynolds number on heat transfer under incompressible flow and forced convection conditions. The air was selected as a working fluid. The inlet temperature of fluid was 283 K. The downstream wall was heated at 313 K. The Reynolds number selected was varied from 200 to 1400. The step height, channel height, and channel width were 0.015 m, 0.030 m, and 0.24 m, respectively. The expansion ratio of the channel was 2. It was obtained from the result of the numerical study that average Nusselt number increases with increasing Reynolds number.

Nowadays, more and more energy is needed to supply the energy of the World due to the developing technologies. Therefore, diversified heat transfer technologies have been set out to be developed. One of them is initiated by using nanofluids that are used for increasing heat transfer. Nanofluids are novel heat transfer fluids having nanoparticles whose sizes change from 1 nm to 100 nm suspended in the base fluids. In recent years, nanofluids have been progressively studied. Kherbeet *et al.* [11] performed nanofluids flow over mixed convection heat transfer in BFS. They used four different nanoparticles (Al_2O_3, CuO, SiO_2, and ZnO). They regarded that ethylene glycol was the base fluid. The nanoparticle diameter was selected 25 nm to 75 nm. Reynolds number was increased from 0.05 to 0.5. The nanoparticle volume fraction was used to 0% to 0.04%. Expansion ratio and step height were selected at 2 μm and 0.96 μm, respectively. They obtained that Nusselt number increases with increasing the volume fraction. Abu-Nada [12] studied numerical investigation of nanofluids for heat transfer increase of separated flows coincidence in a BFS. Five different types of nanoparticle were investigated (Cu, Ag, Al_2O_3, CuO, and TiO_2). Volume fraction was at 0% to 0.2%. The base fluid was pure water. The range of Reynolds number was used 200 to 600. Expansion ratio was designed to 2. The channel was 2-D. He obtained that Reynolds number is independent in re-circulation zone. Selimefendigil and Oztop [13] studied the effect of heat transfer on

pulsating fluids flowing through a corrugated duct with BFS. They only used a type of nanoparticle (CuO) and selected pure water for base fluid. The nanoparticle volume fraction was 2.0%. The range of Reynolds number was 10-200. Expansion ratio was 2. They observed that Nusselt number increases with increasing height and length of the triangle. Ekiciler and Arslan [14] numerically conducted a study of heat transfer and flow characteristics on forced convection laminar flow conditions by using 2-D duct with BFS. The SiO_2-water nanofluid was used as a working fluid. The nanoparticle volume fraction was ranged from 1.0% to 4.0%. Reynolds number was between 75-225. Both of the step and inlet heights of the duct were 4.8 mm. As the downstream wall was subjected to a constant and uniform heat flux of 2000 W/m^2, the other walls were insulated. It was found from the results of the numerical simulation that the Nusselt number increases with increasing the nanoparticle volume fraction. However, there was no significant change in Darcy friction factor. Al-aswadi *et al.* [15] performed laminar nanofluid flow over 2-D BFS. The study was performed by using different nanoparticles (Au, Ag, Al_2O_3, Cu, CuO, diamond, SiO_2, and TiO_2). The base fluid was water. The volume fraction was 5.0%. The range of Reynolds number was 50-175. Step height and expansion ratio were performed 4.8 mm and 2 mm, respectively. In conclusion, the re--circulation size increased with increasing Reynolds number. In addition, they decided that maximum static pressure is obtained for the SiO_2 nanoparticle. Kherbeet *et al.* [16] performed a numerical simulation for heat transfer and flow characteristics in a 2-D duct with microscale backward-facing step (MBFS). The flow was considered at laminar mixed convection condition. Four different nanoparticles types which were ZnO, Al_2O_3, SiO_2, and CuO with the volume fraction of 1.0%, 2.0%, 3.0%, and 4.0% were dispersed in ethylene glycol. The range of Reynolds number and diameter of nanoparticle were at 0.05-0.5 and 25-75 nm, respectively. Duct having a step height of 96 μm and the expansion ratio of 2 was heated downstream of the stepped wall with uniform heat flux. The main aim of the study was the determination of the effect of nanofluids on heat transfer. They noticed that the increase of Reynolds number causes to increase the skin friction coefficient and Nusselt number. They also revealed that the smallest diameter of nanoparticle has the highest Nusselt number. Kherbeet *et al.* [17] carried out numerical and experimental studies under laminar forced convection nanofluids flow over MBFS to observe the effects of nanofluid on heat transfer. The duct's step height was 600 μm and its downstream of the wall was exposed uniform heat flux. The experiment was studied at various Reynolds numbers changed from 280 to 470. In the experimental studies, SiO_2-water and Al_2O_3-water nanofluids were used as working fluids. The diameter of nanoparticle was 30 nm and volume fraction was varied from 0 to 0.01. They compared the experimental results with numerical simulation. It was obtained that the numerical and experimental results were in good agreement. Also, it was found that maximum Nusselt number is obtained by using SiO_2-water nanofluid. Kherbeet *et al.* [18] aimed to clarify the effect of step height on heat and flow characteristics in a 3-D duct with MBFS. The flow was considered as laminar mixed convection condition. Reynolds number was 35. While the downstream stepped wall was heated with the constant heat flux of 12 W/m^2, straight wall temperature was kept at 323 K. The base fluid was ethylene glycol. The SiO_2 nanoparticle with the volume fraction of 4.0% was added to the base fluid. Step heights were 350, 450, and 550 μm. They found that the increasing step height of the duct increases both the Nusselt number and skin friction coefficient.

It is obvious from the elaborated literature review that the case of forced convective heat transfer in a duct having corrugated BFS utilizing different nanoparticle volume fractions of SiO_2-water nanofluid seems has not been investigated in the past and this has motivated the

present study. The SiO_2-water nanofluid has been selected as working fluid due to higher thermal conductivity value of it. The present study deals with 2-D laminar forced convective nanofluid flow over a corrugated duct with BFS. Results of interests such as velocity distribution, Nusselt number, and friction factor were reported to illustrate the effect of nanoparticle volume fraction of nanofluid on these parameters.

Mathematical modeling

Physical model and boundary conditions

Laminar forced convection of the nanofluid in a 2-D aluminum corrugated duct with BFS, which is presented in fig. 1, has been numerically investigated. The length of the upstream and downstream wall was 48 cm and 96 cm, respectively. Total duct height was 9.6 mm. An ellipse wave shape was used for the part of the bottom wall. The height and width of it were 1.2 mm and 9.6 mm, respectively. While the downstream stepped wall was uniformly heated with a constant heat flux of 2000 W/m^2, the other walls were insulated. The nanofluid inlet temperature was 300 K. Solid nanoparticles with size under 100 nm were considered to be able to use single phase approach, thus single-phase approach was practiced for nanofluid modeling and the phase of nanofluid was assumed to be as a continuous [19]. The following assumptions were adopted for this numerical study: both heat transfer and nanofluid flow in duct were in 2-D and steady-state, nanofluid flow was incompressible and laminar flow, the physical properties of nanofluid, such as specific heat, density, and thermal conductivity were taken as temperature independent, negligible viscous dissipation and radiation heat transfer, and the base fluid and the nanoparticles were in thermal equilibrium.

With mentioned assumptions, governing equations of continuity, momentum, and energy are given, respectively:

$$\vec{\nabla}\vec{\mathrm{V}} = 0 \tag{1}$$

$$\rho_{\mathrm{eff}} \frac{D\vec{\mathrm{V}}}{Dt} = -\Delta p + \mu_{\mathrm{eff}} \nabla^2 \vec{\mathrm{V}} \tag{2}$$

$$\rho_{\mathrm{eff}} (c_p)_{\mathrm{eff}} \frac{DT}{Dt} = k_{\mathrm{eff}} \nabla^2 T \tag{3}$$

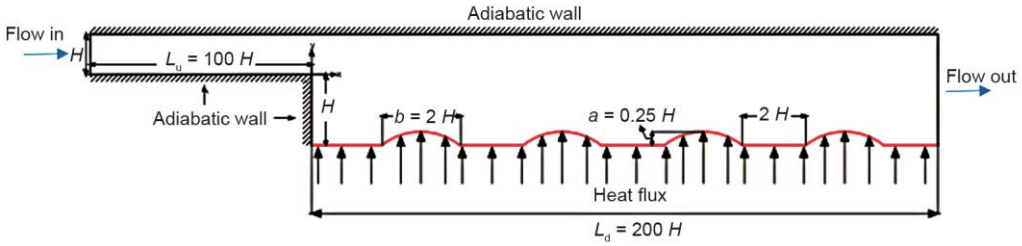

Figure 1. Schematic diagram for corrugated backward facing step

Boundary conditions assuming for the calculation are as follows.

- Upstream condition (inlet) at $x = -L_u$, $0 \le y \le H$; $u = u_i$, $v = 0$, $T = T_i$.
- Downstream exit condition (outlet) at $x = L_d$, $-H \le y \le H$; $P = P_{out}$.
- Straight wall (upper wall) at $-L_u \le x \le L_d$, $y = H$; $u = v = 0$, $\partial T/\partial x = 0$.

– Stepped wall condition:
  – upstream of the step at $-L_u \le x \le 0$, $y = 0$; $u = v = 0$, $\partial T/\partial x = 0$,
  – for the step at $x = 0$, $-H \le y \le 0$; $u = v = 0$, $\partial T/\partial x = 0$, and
  – downstream of the step at $0 \le x \le L_d$, $y = -H$, $u = v = 0$, $q'' = q''_w$.

Calculations of thermophysical properties of nanofluid

Thermophysical properties of the SiO_2 nanoparticle, water, and SiO_2-water nanofluid are given in tab. 1. The magnitude of the volume fraction of nanofluid has been determined from the ratio of the volume of the nanoparticle to the volume of the base fluid.

Table 1. Thermophysical properties of SiO_2-water and its components

Type	ρ [kgm^{-3}]	μ [Nm^{-1}s^{-1}]	k [Wm^{-1}K^{-1}]	c_p [Jkg^{-1}K^{-1}]
Water	996.6	0.000855	0.613	4179
SiO_2 [20]	997	–	1.2	703
SiO_2-water, 1.0%	1009.03	0.000914	0.620	4103.21
SiO_2-water, 2.0%	1021.06	0.000986	0.622	4029.21
SiO_2-water, 3.0%	1033.09	0.001071	0.624	3956.93

The physical properties of nanofluid for different volume fractions are determined as follows.

Vajjha and Das [21] offered the equation of effective thermal conductivity for nanofluid:

$$k_{\text{eff}} = k_{\text{static}} + k_{\text{brownian}} \tag{4}$$

Ghasemi and Aminossadati [22] presented the k_{static} as:

$$k_{\text{static}} = k_{\text{f}} \left[\frac{(k_{\text{s}} + 2k_{\text{f}}) - 2\varphi(k_{\text{f}} - k_{\text{s}})}{(k_{\text{s}} + 2k_{\text{f}}) + \varphi(k_{\text{f}} - k_{\text{s}})} \right] \tag{5}$$

where k_{s} and k_{f} are the thermal conductivities of the solid nanoparticles and the base fluid, respectively.

Vajjha and Das [21] presented thermal conductivity originating from Brownian motion:

$$k_{\text{brownian}} = 5 \cdot 10^4 \beta\varphi\rho_{\text{f}} c_{p,\text{f}} \sqrt{\frac{KT}{\rho_{\text{s}} d_{\text{p}}}} f(T,\varphi) \tag{6}$$

where

$$f(T,\varphi) = \frac{(2.8217 \cdot 10^{-2}\varphi + 3.917 \cdot 10^{-3})T}{T_{\text{r}}} + (-3.0669 \cdot 10^{-2}\varphi - 3.91123 \cdot 10^{-3}) \tag{7}$$

where T is the fluid temperature and taking constant at 300 K, K – the Boltzmann constant, and T_{r} – the reference temperature.

Corcione [23] suggested the equation of effective thermal expansion for nanofluid:

Table 2. The β value of SiO_2 nanoparticles and its boundary conditions

Parameters	Values
β	$1.9526(100\ \varphi)^{-1.4594}$ [11]
Concentration	$1\% \le \varphi \le 3\%$
Temperature	298 K $\le T \le$ 363 K

$$\beta_{\text{eff}} = \frac{(1-\varphi)(\rho\beta)_{\text{f}} + \varphi(\rho\beta)_{\text{s}}}{(1-\varphi)\rho_{\text{f}} + \varphi\rho_{\text{s}}} \tag{8}$$

where β_{s} and β_{f} are the thermal expansion coefficient of nanoparticle and water, respectively. The value of effective thermal expansion coefficient for SiO_2 nanoparticle is given in tab. 2.

Corcione [23] presented viscosity of nanofluid:

$$\frac{\mu_{\text{eff}}}{\mu_{\text{f}}} = \frac{1}{1-34.87\left(\dfrac{d_{\text{p}}}{d_{\text{f}}}\right)^{-0.3}\varphi^{1.03}} \tag{9}$$

where

$$d_{\text{f}} = \left(\frac{6M}{\text{N}\pi\rho_{fo}}\right)^{1/3} \tag{10}$$

where μ_{f} and μ_{eff} are the viscosity of water and nanofluid, respectively, φ is the volume fraction of nanoparticle, d_{f} – the water equivalent diameter, d_{p} – the diameter of the nanoparticle. ρ_{fo} – the mass density of the water calculated at T = 293 K, M – the base fluid's molecular weight, and N – the Avogadro number.

Corcione [23] also proposed the effective density of nanofluid:

$$\rho_{\text{eff}} = (1-\varphi)\rho_{\text{f}} + \varphi\rho_{\text{s}} \tag{11}$$

where ρ_{s}, ρ_{f}, and ρ_{eff} are the densities of the nanoparticle, water, and nanofluid, respectively.

Corcione [23] offered the effective specific heat of nanofluid:

$$(c_p)_{\text{eff}} = \frac{(1-\varphi)(\rho c_p)_{\text{f}} + \varphi(\rho c_p)_{\text{s}}}{(1-\varphi)\rho_{\text{f}} + \varphi\rho_{\text{s}}} \tag{12}$$

where $(c_p)_{\text{f}}$ and $(c_p)_{\text{s}}$ are the specific heat of water and nanoparticle, respectively.

Defining of variables

Average-local Nusselt number, average-local Darcy friction factor, and average-local heat transfer coefficient are calculated:

$$h_x = \frac{q''}{T_{\text{w}} - T_{\text{b}}} \tag{13}$$

$$\text{Nu}_x = \frac{h_x D_{\text{h}}}{k_{\text{eff}}} \tag{14}$$

$$h_{\text{eff}} = \frac{\rho_{\text{eff}} u_{\text{i}} A_{\text{c}} (c_p)_{\text{eff}} (T_{\text{o}} - T_{\text{i}})}{A_{\text{s}} (T_{\text{w}} - T_{\text{m}})} \tag{15}$$

$$\text{Nu} = \frac{h_{\text{eff}} D_{\text{h}}}{k_{\text{eff}}} \tag{16}$$

$$f_x = \frac{8\tau_{\text{o}}}{\rho_{\text{eff}} u_{\text{i}}^2} \tag{17}$$

$$f = \frac{\Delta P \dfrac{D_{\text{h}}}{L}}{\rho_{\text{eff}} \dfrac{u_{\text{i}}^2}{2}} \tag{18}$$

Numerical approach and mesh independence test

In the numerical computations, the finite volume method (FVM) based CFD code was used to determine the numerical calculations. The FVM transforms the governing equations to algebraic equations that can be solved numerically. The convection terms in mass, momentum, and energy equations were discretized using a second order upwind scheme. The SIMPLE algorithm was used to resolve the coupling between velocity and pressure. The Green-Gauss cell-based method was applied for discretization of the momentum and energy equations. To obtain convergence, each equation for mass, momentum, and energy were iterated until the residual less than $1 \cdot 10^{-6}$. No convergence problems were observed during the calculations. The numbers of mesh points or control volumes were increased close to the walls of the duct and near to the BFS to get better accurate results as given in fig. 2.

Figure 2. Computational domain of the problem

The mesh independence test was conducted by increasing the mesh number until the variation in both average friction factor and average Nusselt number were less than 0.1%. To obtain the optimum mesh number, a grid independence study was conducted using thirteen different mesh numbers in the range of $6.05 \cdot 10^3$ -$6.09 \cdot 10^4$ for Re = 240. Changing of average Darcy friction factor and Nusselt number with mesh number for pure water-flow was given in fig. 3. It was observed that a further refinement of mesh number from $1.8 \cdot 10^4$ to $6.09 \cdot 10^4$, the changing of the average Nusselt number and average Darcy friction factor is negligible. Hence, optimum mesh number with minimum computational time and maximum accuracy approximately can be seen at $2.6 \cdot 10^4$ for this study.

To test the accuracy of the numerical simulation, values of pressure drop along the duct were compared with a study, conducted by Al-aswadi *et al.* [15] obtained from the literature, in fig. 4. The results obtained by the present study are good agreement with the study conducted by Al-aswadi *et al.* [15].

Results and discussion

In this section, the effects of nanoparticle volume fraction on velocity distribution, Nusselt number, and Darcy friction factor are investigated under steady-state forced convection laminar SiO_2-water nanofluid flow conditions. In fig. 5, the velocity magnitudes of the

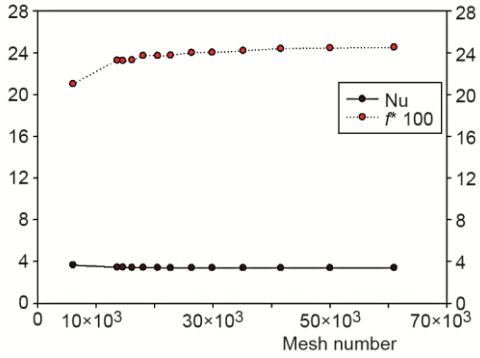

Figure 3. Mesh independence study

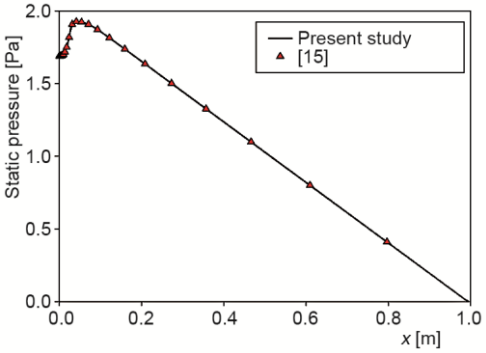

Figure 4. Comparison of the pressure drop of the present study for pure water at Re = 175 with literature

SiO_2-water nanofluids and pure water are investigated at Re = 240 for different locations and volume fractions. The velocity magnitude is totally proportional to the nanoparticle volume fraction. Velocity magnitude increases with increasing the nanoparticle volume fraction. The velocity magnitude of SiO_2-water nanofluid is maximum at 3.0% volume fraction. The velocity magnitude of pure water is minimum. In general, it is seen that the velocity magnitude decreases moving away from the starting point. Figures 5(a) and 5(b) testimony that there is a re-circulation region occurs after the step. Figures 5(c), 5(d), and 5(e) show that the nanofluid flow is independent of the effects of sudden expansion.

The velocity magnitudes of the SiO_2-water nanofluid for different Reynolds numbers are investigated at 3.0% volume fraction under different locations in fig. 6. Velocity magnitude increases with increasing the Reynolds number. The velocity magnitude of SiO_2--water nanofluid is maximum at Re = 240. In general, it is seen the velocity magnitude substantially influences by the Reynolds number. Also, the re-circulation region size becomes smaller as the flow closes to the duct outlet.

In fig. 7, the variation of average Nusselt number with Reynolds number using different nanoparticle volume fractions of SiO_2-water nanofluid is shown. The different nanoparticle volume fractions are seen to affect the average Nusselt number. As the volume fraction and the Reynolds number increases, the average Nusselt number monotonically increases, also. Figure 7 shows that when any Reynolds number is examined, the average Nusselt number reaches a maximum value at % 3.0 volume fraction.

The effect of nanoparticle volume fraction on average Darcy friction factor distribution of SiO_2-water nanofluid and pure water is given in fig. 8. The average Darcy friction factor, which directly affects the pumping power, decreases due to increased velocity and viscosity as the Reynolds number increases at different volume fractions. In addition, average Darcy friction factor does not almost influence by nanoparticle volume fraction. This is an encouraging situation for using SiO_2-water nanofluid when compared to pure water.

The local Nusselt number along the heated wall with different nanoparticle volume fractions and pure water at Re = 240 was presented in fig. 9. It is revealed that local Nusselt number distribution is maximum at just after the step where occurs re-circulation region. Because the nearest bottom surface to the step is cooler than the rest of the bottom surface. So, the local Nusselt number is the highest value at just after the step. Then, it decreases as moving to the outlet of the duct. It increases with increasing SiO_2 nanoparticle volume fraction, also.

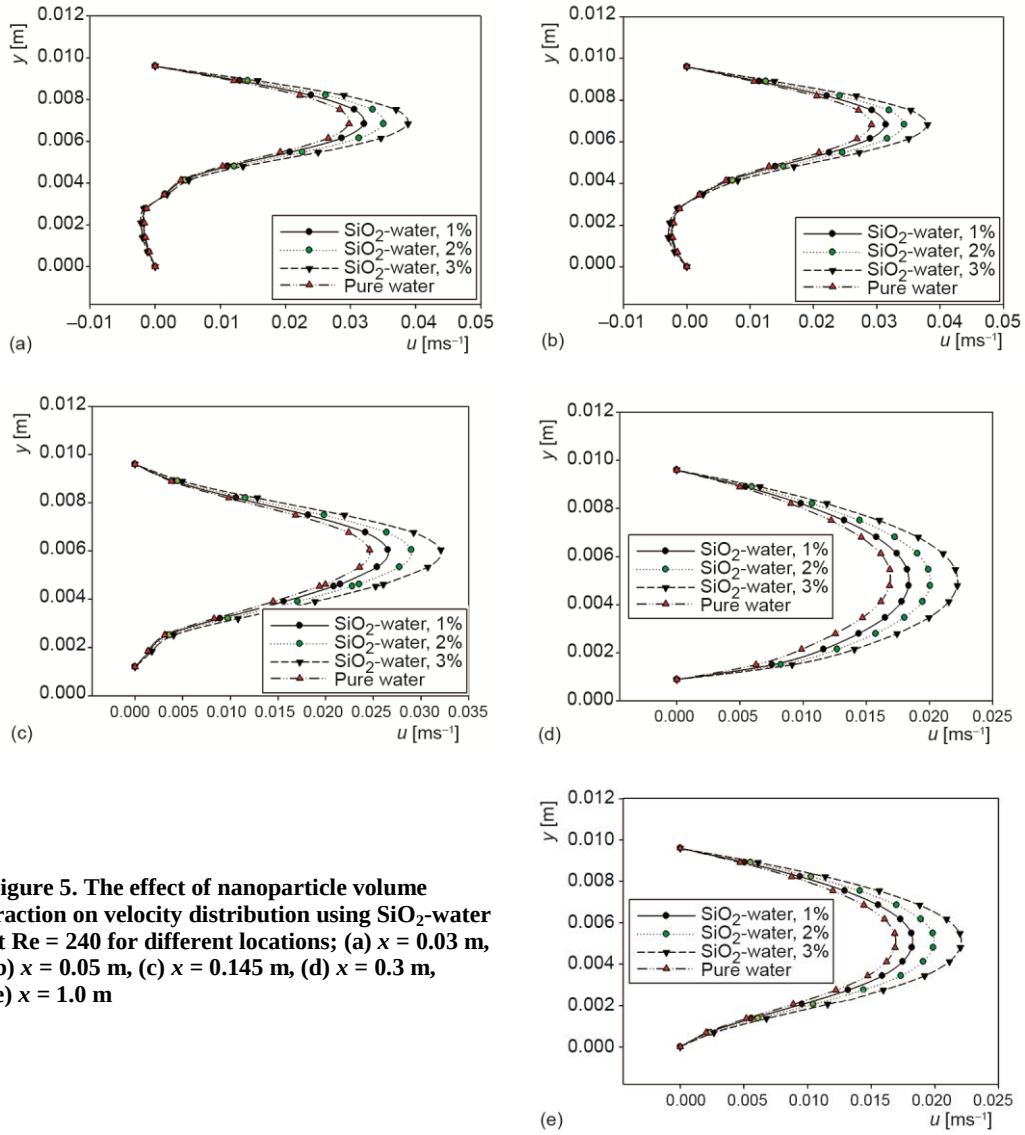

Figure 5. The effect of nanoparticle volume fraction on velocity distribution using SiO_2-water at Re = 240 for different locations; (a) x = 0.03 m, (b) x = 0.05 m, (c) x = 0.145 m, (d) x = 0.3 m, (e) x = 1.0 m

The maximum local Nusselt number can be obtained at 3.0% nanoparticle volume fraction for Re = 240. Furthermore, fluctuations are seen at some points along the heated wall as a result of jumping fluid that causes the thermal boundary-layer thickness getting smaller. Heat trans-

fer coefficient reaches its peak point at these points because of the smaller thermal boundary-layer thickness.

The local Darcy friction factor distribution is illustrated along the heated wall for different nanoparticle volume fractions at Re = 240 in fig. 10. It is noticed that local Darcy friction factor has the lowest value in the re-circulation region due to the lower velocity magnitude and shear stress in it. While the nanofluid passes over the obstacle, there are bounces at the values of local Darcy friction factor. This bounces periodically continue along the bottom wall. Hence, the SiO_2-water nanofluid flow approaches the hydrodynamically fully developed condition. Also, it is realized that the local Darcy friction factor is independent of the nanoparticle volume fraction.

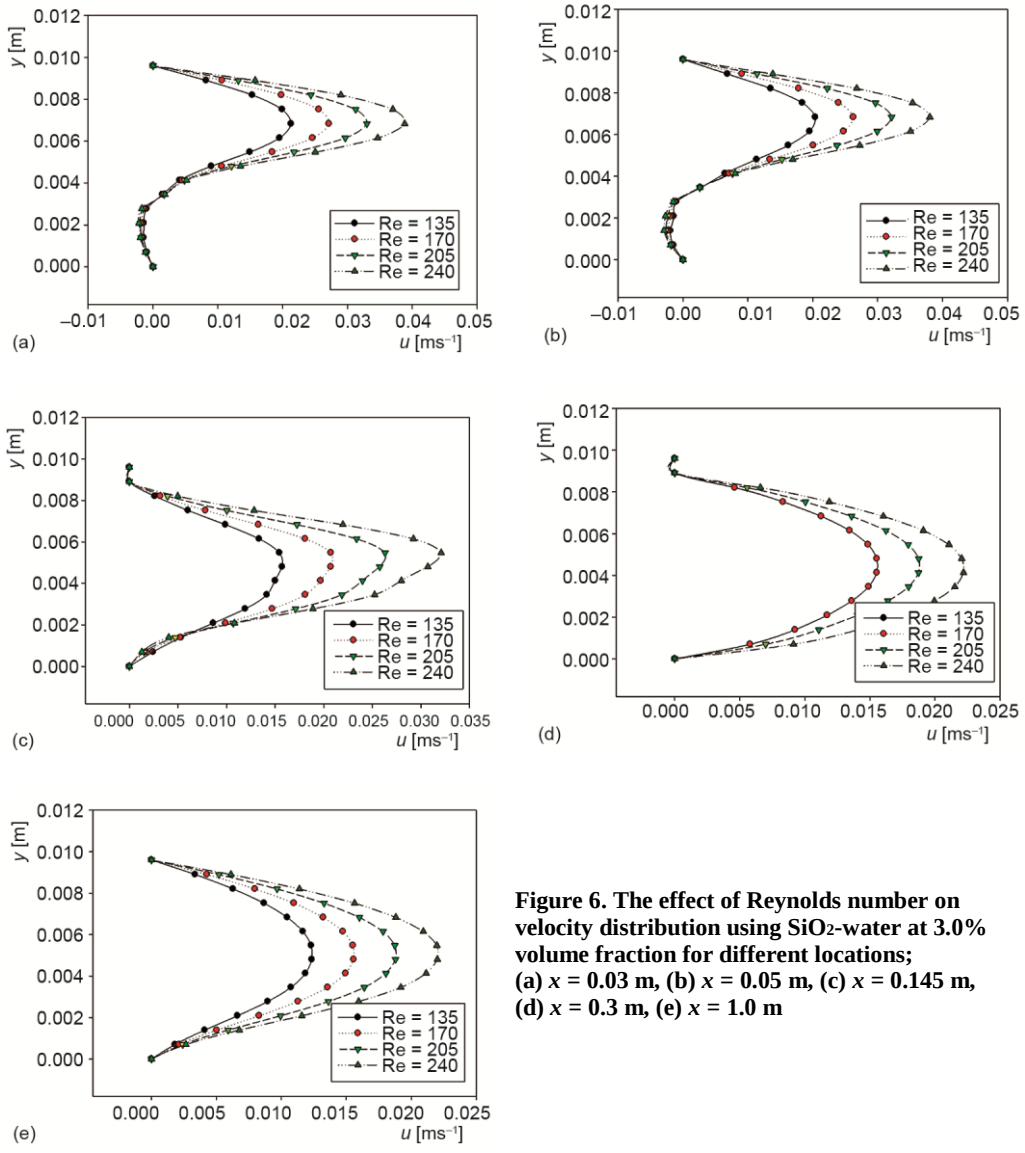

Figure 6. The effect of Reynolds number on velocity distribution using SiO_2-water at 3.0% volume fraction for different locations; (a) x = 0.03 m, (b) x = 0.05 m, (c) x = 0.145 m, (d) x = 0.3 m, (e) x = 1.0 m

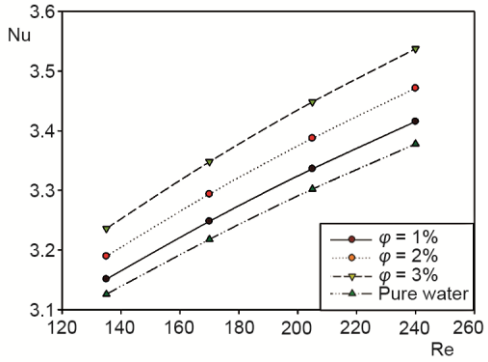

Figure 7. Average Nusselt number distribution using SiO_2-water nanofluid and pure water for different nanoparticle volume fractions

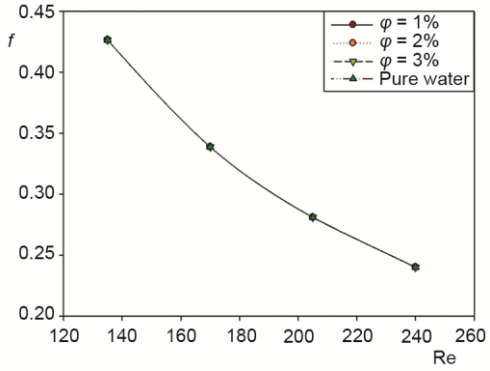

Figure 8. Average Darcy friction factor distribution using SiO_2-water nanofluid and pure water for different nanoparticle volume fractions

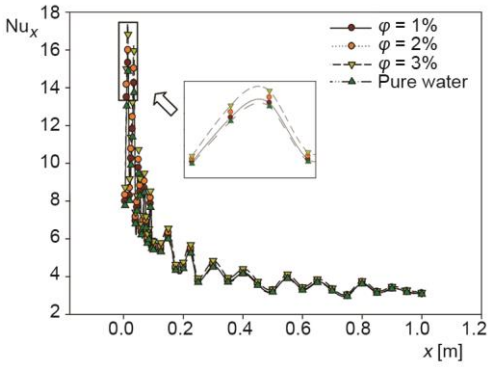

Figure 9. Local Nusselt number distribution using SiO_2-water nanofluid and pure water for different nanoparticle volume fractions at Re = 240

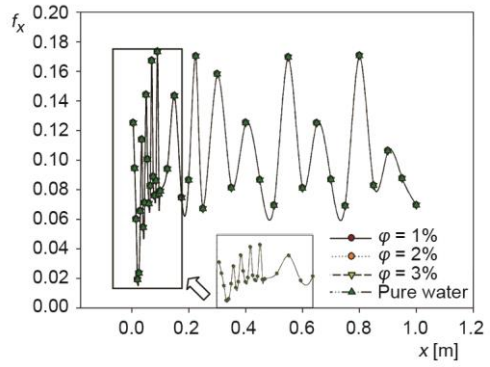

Figure 10. Local friction factor distribution using SiO_2-water nanofluid and pure water for different nanoparticle volume fractions at Re = 240

Conclusion

The SiO_2-water nanofluid flow over 2-D corrugated duct with BFS is simulated under laminar forced convection condition. The obtained results are the following.

The average Nusselt number increases with increasing the Reynolds number and nanoparticle volume fraction. Corrugated section effects the local Nusselt number which reaches the highest and the lowest values.

- The average Darcy friction factor decreases with increasing Reynolds number. There is no effect of changing of nanoparticle volume fractions on it. However, local Darcy friction factor is substantially influenced by the corrugated section.
- The velocity magnitude increases with increasing volume fraction and maximum velocity magnitude is obtained at 3.0% volume fraction.
- Both velocity magnitude and the size of the re-circulation region increase with the increasing Reynolds number.

Nomenclature

A_c – cross-sectional area, [m^2]
A_s – surface area of heated wall, [m^2]
c_p – specific heat, [$Jkg^{-1}K^{-1}$]
D_h – hydraulic diameter, 2 H, [m]
d_p – nanoparticles diameter, [nm]
f – average Darcy friction factor, [–]
H – inlet channel height, [m]
h – convective heat transfer coefficient, [$Wm^{-2}K^{-1}$]
K – Boltzmann constant, [–]
k – thermal conductivity, [$Wm^{-1}K^{-1}$]
L – length of the heated section, [m]
L_u – the length of step, [m]
M – molecular weight, [$kgkmol^{-1}$]
N – Avogadro number, [–]
Nu – average Nusselt number, (= hD_h/k), [–]
P – pressure, [Pa]
q'' – heat flux, [Wm^{-2}]
Re – Reynolds number, (= $\rho u_i D_h/\mu$), [–]
T – fluid temperature, [K]

Greek symbols

β – thermal expansion coefficient, [K^{-1}]
μ – dynamic viscosity, [Nsm^{-2}]
ρ – density, [kgm^{-3}]
τ – shear stress, [Nm^{-2}]
ν – kinematic viscosity, [m^2s^{-1}]
φ – nanoparticle volume fraction, [–]

Subscripts

d – downstream
eff – effective
f – fluid
i – inlet condition
m – mean
o – outlet condition
r – reference
s – solid
u – upstream
x – local

References

[1] Selimefendigil, F., Oztop, H. F., Influence of Inclination Angle of Magnetic Field on Mixed Convection of Nanofluid Flow over a Backward Facing Step and Entropy Generation, *Powder Technology, 26* (2015), 6, pp. 1663-1675
[2] Erturk, E., Numerical Solutions of 2-D Steady Incompressible Flow over a Backward-Facing Step, Part I: High Reynolds Number Solutions, *Computers and Fluids, 37* (2008), 6, pp. 633-655
[3] Saldana, J. G. B., Anand, N. K., Flow over a Three-Dimensional Horizontal Forward-Facing Step, *Numerical Heat Transfer, Part A, 53* (2008), 1, pp. 1-17
[4] Iwai, H., *et al*., Flow and Heat Transfer Characteristics of Backward-Facing Step Laminar Flow in a Rectangular Duct, *International Journal of Heat Mass Transfer, 43* (2000), 3, pp. 457-471
[5] Goldstein, R. J., *et al*., Laminar Separation Reattachment, and Transition of the Flow over a Downstream-Facing Step, *Journal of Basic Engineering, 92* (1970), 4, pp. 732-741
[6] Denham, M. K., Patrick, M. A., Laminar Flow Over a Downstream-Facing Step in a Two-Dimensional Flow Channel, *Trans. Inst. Chem. Eng., 52* (1974), 4, pp. 361-367
[7] Rinoie, K., *et al*., Behaviours of Separated and Reattaching Flow Formed over Backward-Facing Step, *Proceedings*, 21st ICAS Congr., Melbourne, Australia, 1998
[8] Nie, J. H., Armaly, B. F., Three-Dimensional Convective Flow Adjacent to Backward-Facing Step – Effects of Step Height, *International Journal of Heat and Mass Transfer, 45* (2002), 12, pp. 2431-2438
[9] Xie, W. A., Xi, G. N., Fluid Flow and Heat Transfer Characteristics of Separation and Reattachment Flow over a Backward-Facing Step, *International Journal of Refrigeration, 74* (2017), Feb., pp. 177-189
[10] Xu, J. H., *et al*., Effect of Reynolds Number on Flow and Heat Transfer in Incompressible Forced Convection over a 3D Backward-Facing Step, *International Journal of Refrigeration, 79* (2017), July, pp. 164-175
[11] Kherbeet, A. Sh., *et al*., The Effect of Nanofluids Flow on Mixed Convection Heat Transfer over Microscale Backward-Facing Step, *International Journal of Heat and Mass Transfer, 55* (2012), 21-22, pp. 5870-5881
[12] Abu-Nada, E., Application of Nanofluids for Heat Transfer Enhancement of Separated Flows Encountered in a Backward Facing Step, *International Journal of Heat and Fluid Flow, 29* (2008), 1, pp. 242-249
[13] Selimefendigil, F., Oztop, H. F., Forced Convection and Thermal Predictions of Pulsating Nanofluid Flow over a Backward Facing Step with a Corrugated Bottom Wall, *International Communications in Heat and Mass Transfer, 110* (2017), July, 231-247

[14] Ekiciler, R., Arslan, K., Numerical Analysis of SiO_2-Water Nanofluid Flow over Backward Facing Step, *Proceedings*, 5th Inter. Conf. on Engineering and Natural Science, Sarajevo, Bosnia and Herzegovina, 2016, Chapter 2, pp. 330-338
[15] Al-Aswadi, A. A., *et al*., Antonio Campo, Laminar Forced Convection Flow over a Backward Facing Step Using Nanofluids, *International Communications in Heat and Mass Transfer, 37* (2010), 8, pp. 950-957
[16] Kherbeet, A. S., *et al*., The Effect of Nanofluids Flow on Mixed Convection Heat Transfer over Microscale Backward-Facing Step, *International Journal of Heat and Mass Transfer, 55* (2012), 21-22, pp. 5870-5881
[17] Kherbeet, A. S., *et al*., Experimental and Numerical Study of Nanofluid Flow and Heat Transfer over Microscale Backward-Facing Step, *International Journal of Heat and Mass Transfer, 79* (2014), Dec., pp. 858-867
[18] Kherbeet, A. S., *et al*., The Effect of Step Height of Microscale Backward-Facing Step on Mixed Convection Nanofluid Flow and Heat Transfer Characteristics, *International Journal of Heat and Mass Transfer, 68* (2014), Jan., pp. 554-566
[19] Moraveji, M. K, *et al.*, Modeling of Convective Heat Transfer of a Nanofluid in the Developing Region of Tube Flow with Computational Fluid Dynamics, *International Communications in Heat and Mass Transfer, 38* (2011), 9, pp. 1291-1295
[20] Salman, B. H., *et al*., Heat Transfer Enhancement of Nanofluids Flow in Microtube with Constant Heat Flux, *International Communications in Heat and Mass Transf., 39* (2012), 8, pp. 1195-1204
[21] Vajjha, R. S, Das, D. K., Experimental Determination of Thermal Conductivity of Three Nanofluids and Development of New Correlations, *International Journal of Heat and Mass Transfer, 52* (2009), 21-22, pp. 4675-4682
[22] Ghasemi, B., Aminossadati, S. M., Brownian Motion of Nanoparticles in a Triangular Enclosure with Natural Convection, *International Journal of Thermal Sciences, 49* (2010), 6, pp. 931-940
[23] Corcione, M., Heat Transfer Features of Buoyancy-Driven Nanofluids Inside Rectangular Enclosures Differentially Heated at the Sidewalls, *International Journal of Thermal Sciences, 49* (2010), 6, pp. 1536-1546

Paper submitted: October 4, 2018
Paper revised: October 10, 2018
Paper accepted: November 11, 2018